DISTRIBUTION STATEMENT A: Approved for public release; distribution is unlimited.

ROMS and SUNTANS Continued Development and Support of AESOP and NLIWI

Oliver B. Fringer
473 Via Ortega, Room 187
Dept. of Civil and Environmental Engineering
Stanford University
Stanford, CA 94305
phone: (650) 725-6878 fax: (650) 725-9720 email: fringer@stanford.edu

Robert L. Street
473 Via Ortega, Room 259
Dept. of Civil and Environmental Engineering
Stanford University
Stanford, CA 94305
phone: (650) 723-4969 fax: (650) 725-9720 email: street@stanford.edu

Grant Number: N00014-05-1-0294
http://suntans.stanford.edu

LONG-TERM GOALS

Our long-term goal is to develop a parallel ocean simulation tool that is capable of simulating processes on a wide range of scales by coupling two vastly different codes, namely the Regional Ocean Modeling System (ROMS, Shchepetkin and McWilliams (2005)), and the Stanford Unstructured Nonhydrostatic Terrain-following Adaptive Navier-Stokes Simulator (SUNTANS, Fringer *et al.* (2006)). The tool will adaptively nest SUNTANS, an unstructured-grid, coastal-scale code, into ROMS, a curvilinear grid, regional-scale code, in regions where the motions are small-scale and so nonhydrostatic. The nested tool will be applied to study highly nonlinear internal waves in the South China Sea in order to develop an improved understanding of mechanisms that govern their generation, propagation, and dissipation.

OBJECTIVES

In support of the long term goal of developing a two-way nested simulation tool to study the interaction of internal waves with mesoscale currents, our objectives are two-fold. The first is to study internal waves in Monterey Bay in support of the AESOP DRI (Assessing the Effects of Submesoscale Ocean Parameterizations), and the second is to study fundamental internal wave processes in the South China Sea in support of the NLIWI and DRI (Nonlinear Internal Waves Initiative). Because recent work employing separate SUNTANS and ROMS simulations has focused on the California coastal current and internal waves in the Monterey Bay region, the west coast was the obvious choice as the study site for the development of the coupled tool, although the ultimate goal is to apply it to the South China Sea.

Report Documentation Page			Form Approved OMB No. 0704-0188

Public reporting burden for the collection of information is estimated to average 1 hour per response, including the time for reviewing instructions, searching existing data sources, gathering and maintaining the data needed, and completing and reviewing the collection of information. Send comments regarding this burden estimate or any other aspect of this collection of information, including suggestions for reducing this burden, to Washington Headquarters Services, Directorate for Information Operations and Reports, 1215 Jefferson Davis Highway, Suite 1204, Arlington VA 22202-4302. Respondents should be aware that notwithstanding any other provision of law, no person shall be subject to a penalty for failing to comply with a collection of information if it does not display a currently valid OMB control number.

1. REPORT DATE **2009**	2. REPORT TYPE	3. DATES COVERED **00-00-2009 to 00-00-2009**
4. TITLE AND SUBTITLE **ROMS and SUNTANS Continued Development and Support of AESOP and NLIWI**		5a. CONTRACT NUMBER
		5b. GRANT NUMBER
		5c. PROGRAM ELEMENT NUMBER
6. AUTHOR(S)		5d. PROJECT NUMBER
		5e. TASK NUMBER
		5f. WORK UNIT NUMBER
7. PERFORMING ORGANIZATION NAME(S) AND ADDRESS(ES) **Stanford University,Dept. of Civil and Environmental Engineering,473 Via Ortega, Room 187,Stanford,CA,94305**		8. PERFORMING ORGANIZATION REPORT NUMBER
9. SPONSORING/MONITORING AGENCY NAME(S) AND ADDRESS(ES)		10. SPONSOR/MONITOR'S ACRONYM(S)
		11. SPONSOR/MONITOR'S REPORT NUMBER(S)
12. DISTRIBUTION/AVAILABILITY STATEMENT **Approved for public release; distribution unlimited**		
13. SUPPLEMENTARY NOTES		
14. ABSTRACT		
15. SUBJECT TERMS		

16. SECURITY CLASSIFICATION OF:			17. LIMITATION OF ABSTRACT	18. NUMBER OF PAGES	19a. NAME OF RESPONSIBLE PERSON
a. REPORT **unclassified**	b. ABSTRACT **unclassified**	c. THIS PAGE **unclassified**	**Same as Report (SAR)**	**10**	

Standard Form 298 (Rev. 8-98)
Prescribed by ANSI Std Z39-18

APPROACH

The nested simulation tool is a joint effort between Stanford and UCLA to implement a coupled cross scale system comprised of the Regional Oceanic Model System (ROMS) and the local scale code SUNTANS (Stanford Unstructured Nonhydrostatic Terrain-following Adaptive Navier-Stokes Simulator). SUNTANS is an unstructured-grid, z-level, parallel coastal ocean simulation tool that solves the Navier-Stokes equations under the Boussinesq approximation with a large-eddy simulation of the resolved motions (Fringer *et al.*, 2006), while ROMS is a curvilinear- and sigma-coordinate regional simulation tool (Shchepetkin & McWilliams, 2005) that now has a nonhydrostatic module (Kanarska et al., 2006). We are developing a novel dual adaptive scheme to simulate scales that range from meters to hundreds of kilometers by coupling the multi-physics and multi-scale simulation tools ROMS and SUNTANS. ROMS will be statically nested within itself, and adaptive SUNTANS grids will be nested within ROMS and refined based on traditional tolerance criteria (i.e. vorticity and density gradients) as well as the nonhydrostatic pressure, which is a good measure of short-wavelength behavior that requires high resolution if it is to be computed accurately.

We are developing the nested tool using simulations of the California Coastal Current by nesting SUNTANS grids in the vicinity of Monterey Bay inside ROMS simulations of the entire U. S. west coast. These simulations focus on the regional currents as well as internal waves in Monterey Bay, in support of the AESOP DRI. In addition to developing the ROMS-SUNTANS tool in this domain, we are testing turbulence models that incorporate the large-eddy simulation framework. These will be used to test the effects of submesoscale parameterizations on currents and internal waves in Monterey Bay. The high-resolution simulations of Monterey Bay will be used to compute the internal wave energy flux and energy flux divergence in order to aid in deciding on an appropriate study site for the field component of the AESOP DRI.

While the nested simulation tool is under development for the U.S. west coast in conjunction with simulations of internal waves in Monterey Bay in support of the AESOP DRI, our work also supports the NLIWI DRI by performing simulations in the South China Sea using SUNTANS to study the generation and propagation of internal solitary waves. The ultimate goal will be to nest these SUNTANS simulations inside ROMS using the ROMS-SUNTANS nested simulation tool.

WORK COMPLETED

We have performed simulations of internal waves in Monterey Bay with high resolution and have evaluated the energy budget in the region. We have also derived the equations governing the detailed energy budget for baroclinic tides, including a detailed investigation of the different forms of evaluating the available potential energy. In the South China Sea, we have analyzed the data from our three-dimensional simulations to determine the generation sites of the nonlinear internal waves in the Sea.

RESULTS

Internal waves in Monterey Bay

We have performed a detailed analysis of the internal wave energy flux in Monterey Bay following the work of Jachec et al. (2007), in which the simulations were performed in a domain that is smaller than the one depicted in Figure 1. Our new domain extends eight internal tidal wavelengths (with respect to propagation in the deep region of the domain) offshore and four to the north and south of the domain. This enables the internal tides to freely radiate away from the topography without being affected by the boundaries. Upon comparison of the modeled barotropic currents to the observations of Klymak (2009), low-frequency currents are evident in the field data that are not present in the model, as depicted in Figure 2, since the model is forced exclusively by the barotropic currents at the boundaries. However, as depicted in Figure 3, agreement between the predictions and observations is excellent after application of a high-pass filter to remove the low-frequency currents.

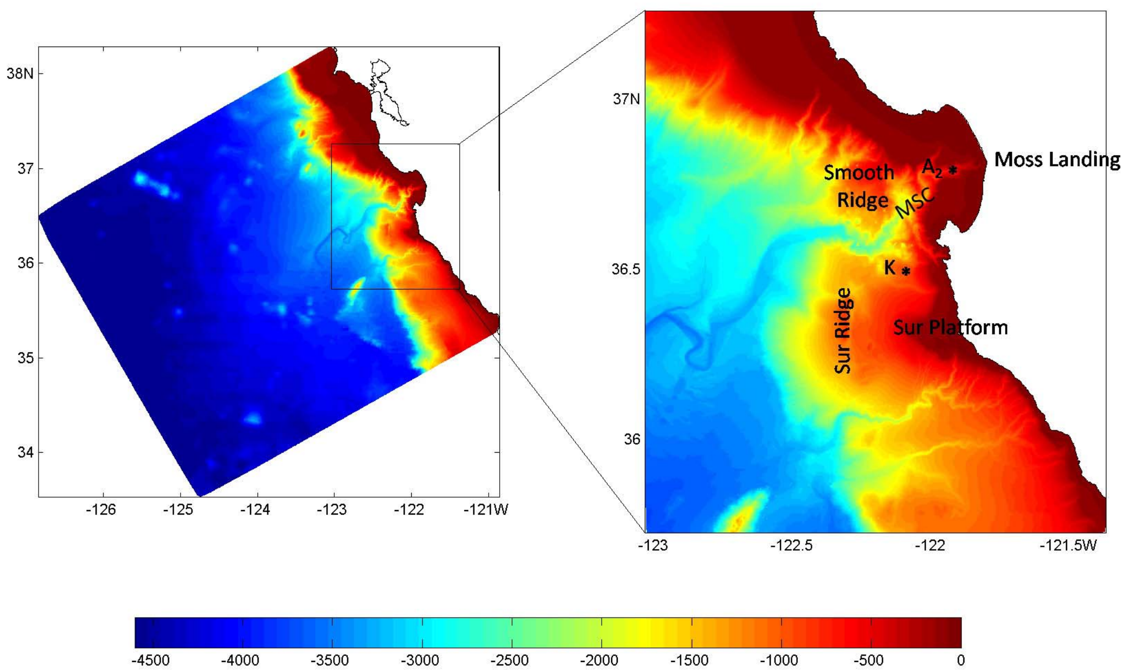

Figure 1: Extended domain of Monterey Bay, with a zoomed-in view of the Bay indicating the locations of moorings A2 and mooring K of Klymak (2009).

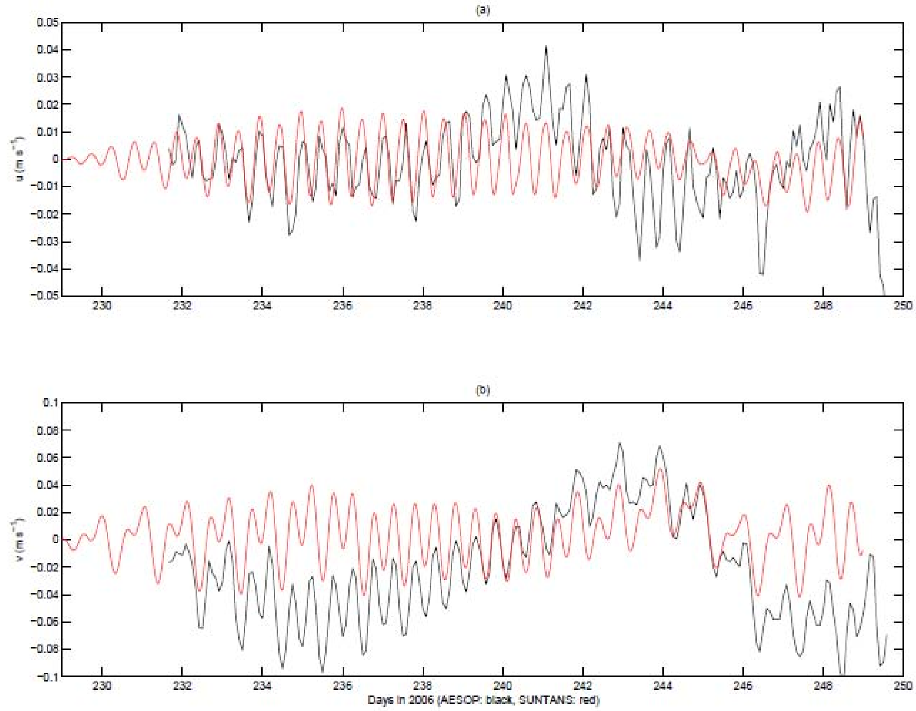

Figure 2: Comparison of (a) cross-shore and (b) along-shore depth-averaged velocity between SUNTANS (red) and observations (black) at station K.

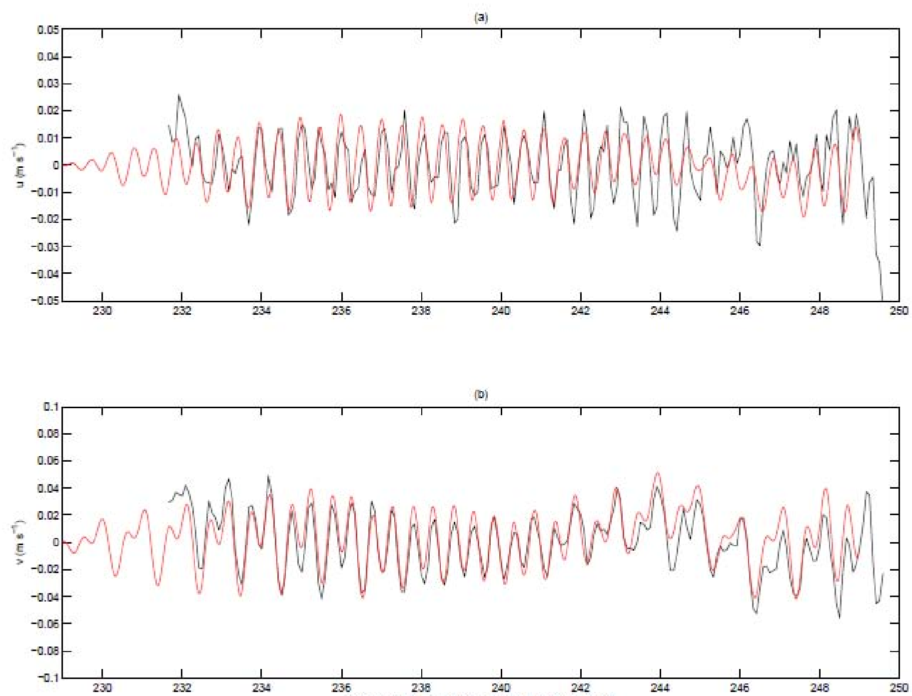

Figure 3: Same as Figure 2, except the observations have been high-pass filtered to remove the low-frequency currents.

The equations governing the evolution of the total (kinetic + potential) baroclinic energy, *E'*, and barotropic energy, E_0, are given by (see, e.g. Carter et al. 2008)

$$\frac{\partial E'}{\partial t} + \nabla_H \cdot \vec{F}' = g\overline{\rho' W} - \varepsilon' + N' + C' \tag{1}$$

$$\frac{\partial E_0}{\partial t} = -g\overline{\rho' W} - \varepsilon_0 + N_0 + C_0 , \tag{2}$$

where $\vec{F}'$ is the depth-integrated baroclinic energy flux (Kunze et al. 2002), $g\overline{\rho' W}$ is the rate at which energy is converted from the barotropic to the baroclinic internal tides (*W* is the barotropic vertical velocity which is linear in the vertical coordinate), and ε is the dissipation. In equations (1) and (2), N and C represent the non-conservative and conservative terms, respectively, in the energy budget, and subscript 0 indicates that the term alters the barotropic energy, while the prime implies that it alters the baroclinic energy. Time-averaging the baroclinic equation (2) shows that, in steady-state (with $\langle \ \rangle$ as the time-averaging operator), the approximate form of the energy budget is given by

$$\nabla_H \cdot \left\langle \vec{F}' \right\rangle = g\left\langle \overline{\rho' W} \right\rangle - \left\langle \varepsilon' \right\rangle , \tag{3}$$

or

$$Flux\,Divergence = Conversion - Dissipation\ , \tag{4}$$

which is obtained by assuming that the other terms, such as nonlinear or nonhydrostatic energy flux, unsteadiness, and cross-terms resulting from depth-averaged correlations in primed quantities, are small, which is a good approximation unless nonlinear and nonhydrostatic waves are present (Venayagamoorthy and Fringer, 2005). Equation (4) implies that the divergence of the internal wave energy flux is in balance with the rate at which energy is being converted from the barotropic tides and dissipation. Figure 4 depicts the energy flux vectors and magnitude as well as the conversion of barotropic to baroclinic energy. In general, conversion is high where the energy flux divergence is high, the difference between the two implying local dissipation (not shown). Red regions in the conversion plot indicate where barotropic energy is converted to baroclinic energy, while blue regions either imply conversion of the opposite sense, but likely result from errors in the calculation since it is unlikely that significant energy is converted from the baroclinic to barotropic tides. The left panel in Figure 4 depicts five regions of elevated internal wave activity. Each region has elevated internal wave energy due to the elevated generation of energy over topography, as implied by the conversion depicted in the right panel. The North Shelf break and Davidson Seamount regions radiate a significant portion of energy into the open ocean, while the energy generated in Monterey Submarine Canyon (MSC) is likely lost locally. It is not clear whether energy generated in the Sur Platform region radiates into the open ocean or is lost locally, nor is it clear where the elevated energy in the Open Ocean region originates. We are in the process of evaluating these details to determine the ultimate fate of the energy that is lost from the barotropic tides in the region.

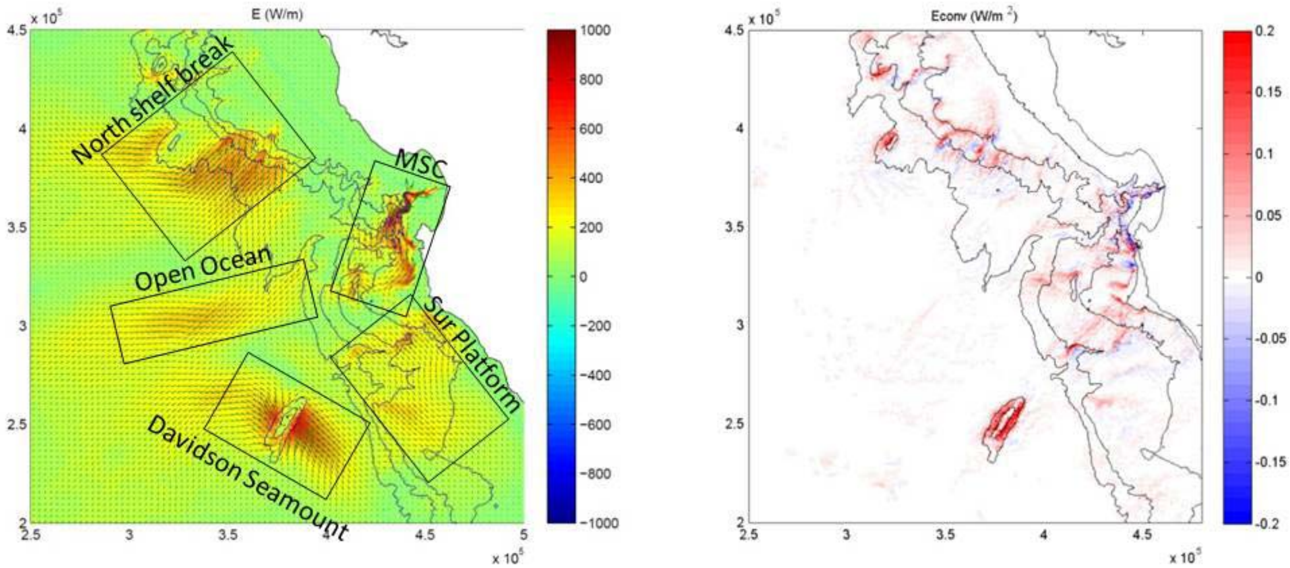

Figure 4: Energy flux in W/m (left) and barotropic-to-baroclinic conversion in W/m^2 (right) in Monterey Bay. The boxes in the left panel highlight different regions of elevated internal wave activity.

Nonlinear internal waves in the South China Sea

Our focus has been on analyzing the results from three-dimensional simulations of internal waves in the South China Sea to determine the generation site of the observed internal waves. Our analysis has shown that reproduction of the observed internal wave field requires accurate simulation of the observed barotropic currents at the hypothesized generation sites. Figure 5 depicts a comparison of the simulated to observed barotropic currents at mooring L1 (see Figure 6) and shows that the phasing predicted by SUNTANS is correct although the amplitude is underpredicted. As expected, the OTIS tidal currents are underpredicted but these can be corrected using more accurate bathymetry. The mismatch between the SUNTANS and observed currents may be due to inaccurate bathymetry or to strong baroclinicity at mooring L1 which creates strong bottom currents relative to the barotropic depth-average. The observations may reflect this strong bottom current because they are taken as the average from a depth of 450 m to 380 m. Nevertheless, the magnitude of the predicted currents is sufficient to generate the observed internal wave signal at mooring B1 (not shown, but included in Annual Report for FY08).

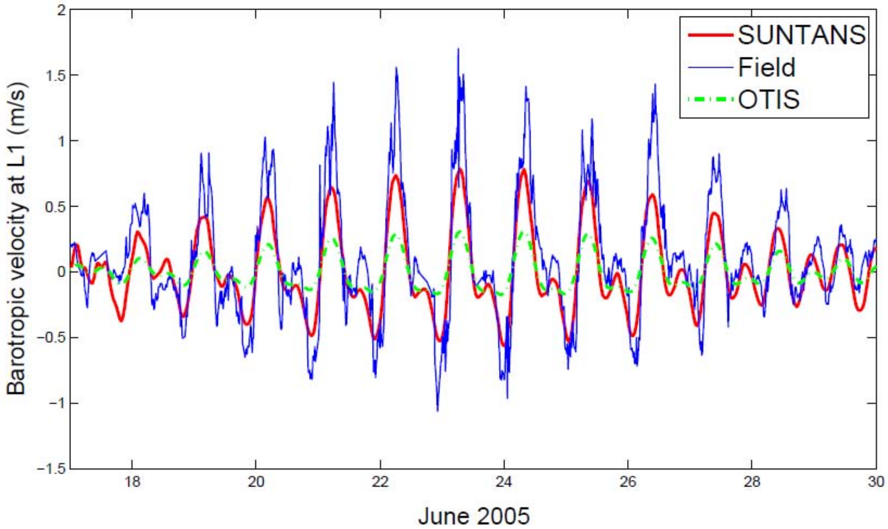

Figure 5: Comparison of barotropic currents at mooring L1 from observations (blue solid thin line), SUNTANS (red solid thick line) and OTIS (green dashed line) during June 17 to June 30, 2005. Positive currents indicate ebb tide towards the Pacific Ocean. The observed currents are the average over the water column extending from -450 m to -380 m.

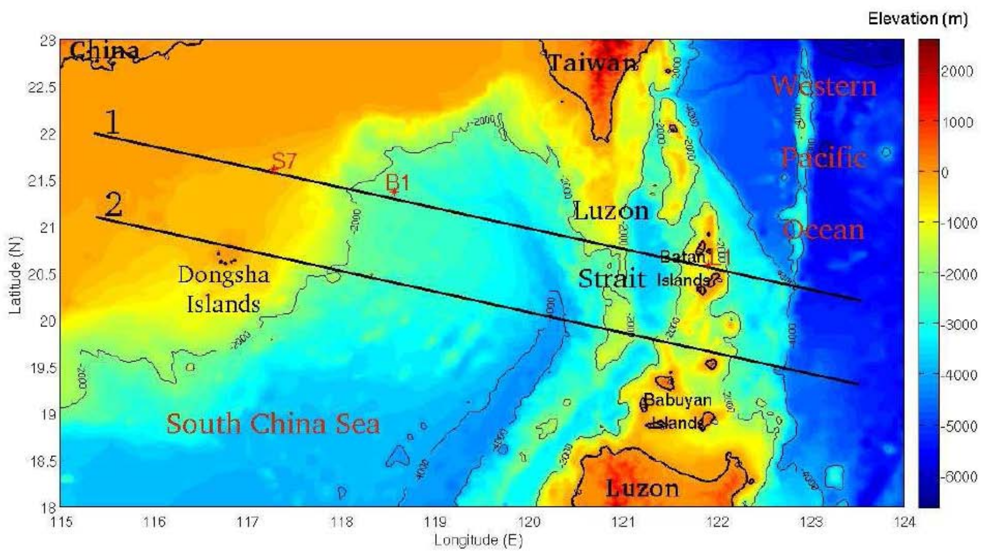

Figure 6: Bathymetry map of the South China Sea, showing the locations of mooring sites L1, B1 and S7 from the WISE/VANS project in 2005. Transect 1 is referred to in Figure 7.

Figure 7 depicts a Hovmoller diagram of the free-surface signature of internal waves propagating across transect 1 in Figure 6. To accentuate individual internal wave peaks, the east-west gradient in the free-surface is plotted as this removes the tidal variability in the free-surface as the tide propagates through the Luzon Strait. Superimposed over the diagram are characteristics following A- and B-wave peaks as they cross mooring B1. The A-waves are those that arrive at mooring S7 every 24 hours and are generated by the diurnal tide, while the B-waves arrive approximately one hour later each day and are generated by the semidiurnal tide (Ramp et al. 2004). Although it is difficult to trace the B-wave characteristics backward in time because the B-waves are not evident in deeper water, the A-wave characteristics are clear and can be traced back to the Eastern ridge at L1. Figure 7 shows that the A-waves take 33 hours to propagate from mooring L1 to mooring B1, which agrees with the finding of Ramp et al. (2004). Furthermore, the analysis shows that the A-wave characteristics cross the ridge at L1 during peak eastward, or ebb, tides. This is also in agreement with Ramp et al.

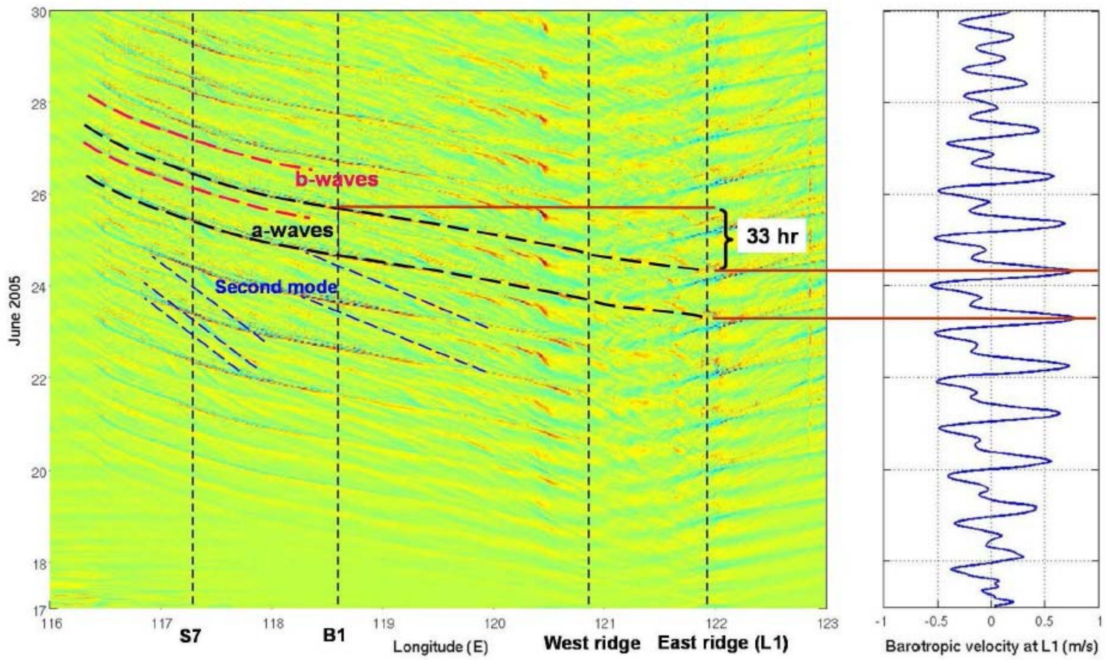

Figure 7: Hovmoller diagram (left panel) of the free-surface gradient along Transect 1 in Figure 6. The locations of the two ridges in the Luzon Strait, and mooring sites B1 in the basin and S7 on the shelf are shown by the vertical black dashed lines. The curved dashed lines indicate the paths of the A-waves in black, B-waves in red, and second-mode waves in blue. The right panel is the barotropic velocity at L1 with positive currents toward the Pacific Ocean.

IMPACT/APPLICATIONS

High-resolution simulations using nonhydrostatic models like SUNTANS and the coupled ROMS-SUNTANS model are crucial for understanding multiscale processes that are unresolved, and hence parameterized, in larger-scale models.

REFERENCES

Carter, G. S., Merrifield, M. A., Becker, J. M., Katsumata, K., Gregg, M. C., Luther, D. S., Levine, M. D., Boyd, T. J., and Y. L. Firing, 2008, Energetics of M2 Barotropic-to-Baroclinic Tidal Conversion at the Hawaiian Islands, J. Phys. Oceanogr., 38 (10), 2205–2223.

Fringer, O. B., Gerritsen, M., and R. L. Street, 2006, An unstructured-grid, finite-volume, nonhydrostatic, parallel coastal ocean simulator, Ocean Modelling, 14 (3-4), 139-278, doi:10.1016/J.OCEMOD.2006.03.006.

Jachec, S. M., Fringer, O. B., Gerritsen, M. G., and R. L. Street, 2006, Numerical simulation of internal tides and the resulting energetics within Monterey Bay and the surrounding area, Geophys Res. Lett., 33, L12605, doi:10.1029/2006GL026314.

Kanarska, Y., Shchepetkin, A., and J. C. McWilliams, 2007, Algorithm for non-hydrostatic dynamics in the Regional Oceanic Modeling System, Ocean Modelling, 18 (3-4), 143-174.

Klymak, J. M., 2009, personal communication.

Kunze, E., Rosenfeld, L. K., Carter, G. S., and M. C. Gregg, 2002, Internal waves in Monterey Submarine Canyon, J. Phys. Oceanogr., 32, 1890-1913.

Ramp, S. R., Tang, T. Y., Duda, T. F., Lynch, J. F., Liu, A. K., Chiu, C.-S., Bahr, F., Kim, H.-R., and Y. J. Yang, 2004, Internal solitons in the northeastern South China Sea part I: Sources and deep water propagation, IEEE J. Oceanic Eng., 29, 1157-1181.

Shchepetkin, A. F., & McWilliams, J.C., 2005, The Regional Oceanic Modeling System: A split-explicit, free-surface, topography-following-coordinate ocean model. *Ocean Modelling*, 9, 347–404.

Venayagamoorthy, S. K., and O. B. Fringer, 2005. Nonhydrostatic and nonlinear contributions to the energy flux budget in nonlinear internal waves, Geophys. Res. Lett., 32, L15603, doi:10.1029/2005GL023432

PUBLICATIONS

Barad, M. F. and O. B. Fringer, 2009, Numerical simulation of shear instabilities in interfacial gravity waves, J. Fluid Mech., in press.

O. B. Fringer, 2008, Nonhydrostatic effects of internal solitary-like waves and possible parameterizations for hydrostatic models, American Geophysical Union, Fall Meeting 2008, abstract #OS51F-08.

Fringer, O. B., and M. F. Barad, 2009, Large-eddy simulation of coherent flow structures in a river, DOD HPCMP Users Group Conference.

Fringer, O.B., 2009, Towards nonhydrostatic ocean modeling with large-eddy simulation, Oceanography in 2025 workshop, California Academy of Sciences (invited).

Fringer, O.B. and M. F. Barad, 2009, Numerical simulation of shear instabilities in interfacial gravity waves, The 4th Warnemünde Turbulence Days (WTD) on Internal Waves and Turbulence in Coastal Seas (invited).

HONORS/AWARDS/PRIZES

Oliver B. Fringer, Presidential Early Career Award, 2009.

Robert L. Street, Distinguished Member of ASCE, 2009.